

The development of cephalic armor in the tokay gecko (Squamata: Gekkonidae: *Gekko gecko*)

Rebecca J. Laver¹  | Cristian H. Morales^{2,3}  | Matthew P. Heinicke⁴  |
 Tony Gamble^{5,6,7}  | Kristin Longoria²  | Aaron M. Bauer⁸  | Juan D. Daza² 

¹Research School of Biology, Australian National University, Canberra, Australia

²Department of Biological Sciences, Sam Houston State University, Huntsville, Texas

³Department of Biology, University of Texas at Arlington, Arlington, Texas

⁴Department of Natural Sciences, University of Michigan-Dearborn, Dearborn, Michigan

⁵Department of Biological Sciences, Marquette University, Milwaukee, Wisconsin

⁶Milwaukee Public Museum, Milwaukee, Wisconsin

⁷Bell Museum of Natural History, University of Minnesota, Saint Paul, Minnesota

⁸Department of Biology, Villanova University, Villanova, Pennsylvania

Correspondence

Juan D. Daza, Department of Biological Sciences, Sam Houston State University, Huntsville, TX.

Email: juand.daza@gmail.com

Funding information

Division of Environmental Biology, Grant/Award Numbers: DEB1555968, DEB1657527, DEB1657656, DEB1657662

Abstract

Armored skin resulting from the presence of bony dermal structures, osteoderms, is an exceptional phenotype in gekkotans (geckos and flap-footed lizards) only known to occur in three genera: *Geckolepis*, *Gekko*, and *Tarentola*. The Tokay gecko (*Gekko gecko* LINNAEUS 1758) is among the best-studied geckos due to its large size and wide range of occurrence, and although cranial dermal bone development has previously been investigated, details of osteoderm development along a size gradient remain less well-known. Likewise, a comparative survey of additional species within the broader *Gekko* clade to determine the uniqueness of this trait has not yet been completed. Here, we studied a large sample of gekkotans (38 spp.), including 18 specimens of *G. gecko*, using X-rays and high-resolution computed tomography for visualizing and quantifying the dermal armor *in situ*. Results from this survey confirm the presence of osteoderms in a second species within this genus, *Gekko reevesii* GRAY 1831, which exhibits discordance in timing and pattern of osteoderm development when compared with its sister taxon, *G. gecko*. We discuss the developmental sequence of osteoderms in these two species and explore in detail the formation and functionality of these enigmatic dermal ossifications. Finally, we conducted a comparative analysis of endolymphatic sacs in a wide array of gekkotans to explore previous ideas regarding the role of osteoderms as calcium reservoirs. We found that *G. gecko* and other gecko species with osteoderms have highly enlarged endolymphatic sacs relative to their body size, when compared to species without osteoderms, which implies that these membranous structures might fulfill a major role of calcium storage even in species with osteoderms.

KEY WORDS

comparative anatomy, CT scans, endolymphatic sac, osteoderms, osteology, reptiles

1 | INTRODUCTION

Acquisition of mineralized integumentary structures – osteoderms – has occurred independently several times in multiple vertebrate lineages (Vickaryous & Sire, 2009). Osteoderms may form as a continuous or patchy layer of osseous tissue in the dermis (Vickaryous & Sire, 2009), and are developed in representatives of most major tetrapod

lineages (both extinct and living; Hill, 2005; Moss, 1969; Romer, 1956) including frogs (e.g., Batista et al., 2014; Campos, Da Silva, & Sebben, 2010; Ruibal & Shoemaker, 1984), dinosaurs (e.g., Curry Rogers, D'emic, Rogers, Vickaryous, & Cagan, 2011; Farlow, Thompson, & Rosner, 1976), leatherback turtles (in contrast to other Testudines; Chen, Yang, & Meyers, 2015), crocodilians (e.g., Seidel, 1979; Sun & Chen, 2013), lizards (e.g., Broeckhoven, Diedericks, & Mouton, 2015;

Broeckhoven, El Adak, Hui, Van Damme, & Stankowich, 2018; Broeckhoven, Mouton, & Hui, 2018; Stanley, Paluh, & Blackburn, 2019), xenarthrans (e.g., Chen et al., 2011; Krmpotic et al., 2015; Vickaryous & Hall, 2006), the fossil Eocene elephant shrew *Pholidocercus* (von Koenigswald & Storch, 1983), and mice of the genus *Acomys* (Kraft, 1995; Niethammer, 1975).

Among squamates, osteoderms have been reported in representatives of almost every major lizard clade (Broeckhoven, du Plessis, Minne, & Van Damme, 2019; Camp, 1923; Conrad, 2008; Estes, de Queiroz, & Gauthier, 1988; Evans, 2008; Gadow, 1901; Gao & Norell, 2000; Moss, 1969; Schmidt, 1912), including iguanians (e.g., de Queiroz, 1987; Schucht, Rühr, Geier, Glaw, & Lambertz, 2019; Siebenrock, 1893), gekkotans (e.g., Levrat-Calviac, 1986; Levrat-Calviac & Zylberberg, 1986; Paluh, Griffing, & Bauer, 2017; Scherz, Daza, Köhler, Vences, & Glaw, 2017; Vickaryous, Meldrum, & Russell, 2015; Villa, Daza, Bauer, & Delfino, 2018), scincoides (e.g., King, 1964; Krause, Evans, & Gao, 2003; Oliver, 1951; Paluh & Bauer, 2017), lacertoideans (e.g., Arnold, 1989; Barahona & Barbadillo, 1998; Bellairs & Kamal, 1981; Costantini, Alonso, Moazen, & Bruner, 2010; Read, 1986; Siebenrock, 1894), and anguimorphs (e.g., Bever, Bell, & Maisano, 2005; Bhullar & Bell, 2008; Conrad, Head, & Carrano, 2014; Maisano, Bell, Gauthier, & Rowe, 2002; McDowell & Bogert, 1954; Zylberberg & Castanet, 1985). Despite this diverse representation however, osteoderms can be inconsistently expressed within clades, even within the same genus (e.g., *Abronia*, Good & Schwenk, 1985; *Varanus*, Erickson, De Rieques, De Buffrénil, Molnar, & Bayless, 2003; and *Gekko*, Vickaryous et al., 2015). Varanids are a particularly contrasting group; for instance, species can exhibit conspicuous osteoderms (*Varanus* [*Megalania*] *priscus* [*prisca*], Erickson et al., 2003; *Varanus komodoensis* OUWENS 1912, Maisano, Laduc, Bell, & Barber, 2019), or lack these dermal structures completely (the vast majority of species within the genus *Varanus*; Auffenberg, 1981; Erickson et al., 2003).

Gekkota, the likely sister clade to all other squamates (Burbrink et al., 2019; Simoes et al., 2018), is a highly diverse group with over 1,900 species (Bauer, 2013; Conrad, 2008; Uetz, Freed, & Hošek, 2019). Despite the high species-richness however, osteoderms have only evolved in three genera of gekkotans, each representing an independent derivation: within the phyllodactylid genus *Tarentola* (Bauer & Russell, 1989; Levrat-Calviac, 1986; Levrat-Calviac & Zylberberg, 1986; Loveridge, 1947; Otto & Coburg, 1909; Parker & Taylor, 1942; Vickaryous et al., 2015; Villa et al., 2018) and two gekkonid genera, *Gekko* (specifically, *G. gecko* LINNAEUS 1758; Daza, Mapps, Lewis, Thies, & Bauer, 2015; Vickaryous et al., 2015) and *Geckolepis* (Paluh et al., 2017; Schmidt, 1911, 1912). Likely due to their independent origins, osteoderms in these genera are different in morphology. In the case of *Tarentola*, the osteoderms even develop a special kind of tissue called osteodermine (Vickaryous et al., 2015). Although discovery of osteoderms in the genus *Geckolepis* was based on early reports in an unidentified specimen (Schmidt, 1911, 1912), until recently it had been a matter of contention as to whether these structures were indeed true osteoderms (Bauer & Russell, 1989; Paluh et al., 2017; Vickaryous et al., 2015). *Geckolepis* also represents a unique situation since a large portion of the skin in these geckos can

be lost at once, degloving the body by an extensive avulsion (Angel, 1942; Paluh et al., 2017; Scherz et al., 2017).

The type genus of the family Gekkonidae, the genus *Gekko*, is undergoing reorganization (Wood et al., 2019) involving division into new subgenera and subsumption of two other genera into *Gekko*. In contrast to *Geckolepis* and *Tarentola*, where osteoderms have been documented across the respective genera, osteoderms in *Gekko* are only known to occur in *Gekko gecko*. However, it is only in recent years that works have begun to describe the ontogenetic development of gecko osteoderms in detail (e.g., Vickaryous et al., 2015), and confidently confirmed osteoderms in additional species (Paluh et al., 2017). In light of this, and with the enhanced ability to visualize the patterning of osteodermal structures *in situ* using high-resolution computed tomography (HRCT) methods (e.g., Maisano et al., 2019), the timing seems apt to reconsider osteoderm presence and development within the revised *Gekko* genus. We have obtained morphological data for a broad taxonomic sampling of species across the *Gekko* group that allows us to explore in detail the occurrence of these rare integumentary elements within this group.

Osteoderms may contribute to a variety of possible functions, including playing a role in protection, locomotion, thermoregulation, and even calcium mineral storage (e.g., Broeckhoven, du Plessis, & Hui, 2017; Buchwitz, Witzmann, Voigt, & Golubev, 2012; Dacke et al., 2015; Farlow, Hayashi, & Tattersall, 2010). Although work is still progressing to understand the complexity of the roles of osteoderms, the distribution and form of these structures across the body may provide some clues. *G. gecko* possesses another structure that is presumed to play a role in calcium storage, the endolymphatic sacs. Endolymphatic sacs are gland-like, contain calcareous substances, and are typically located in the cranial vault, proximal to the brain (e.g., Bauer, 1989; Kluge, 1967; Whiteside, 1922). Although the full function of the endolymphatic system remains to be determined, it has been hypothesized to be involved in aspects of inner ear pressure regulation, sound transmission, protection of the central nervous system, and storage of calcium for both reproductive functions and for bone formation (Bauer, 1989; Kluge, 1967; Mangione & Montero, 2001). In certain iguanids, agamids, chameleons, and several gekkotans, the endolymphatic sacs are expanded to the point that they protrude anteriorly from the cranial vault and/or posteriorly to lie on either side of the neck (Bauer, 1989; Kluge, 1967). In *G. gecko* the extracranial endolymphatic sacs are particularly enlarged (Kluge, 1967), and we suspect this may serve for calcium storage not only to supply extra material for both reproductive functions and for bone formation, but additionally for osteoderm production. As a first step in investigating the possibility of a relationship between these structures, we also measured the size of extracranial endolymphatic sacs in a broad sampling of geckos to quantify the relationship between osteoderm presence and size of endolymphatic sacs.

The ontogenetic development of osteoderms in *G. gecko* was previously described by Vickaryous et al. (2015) together with geckos of the genus *Tarentola*. Previously, the ontogenetic development of the skull was studied in *G. gecko*, but as this work was based on skeletonized specimens, the osteoderms were not included (Daza et al., 2015). In this article, we had three broad aims and used HRCT-images to document in further detail the development of osteoderms in a series of postnatal

individuals of different size of the species *G. gecko*. This imaging technique allows us to: (a) visually document in detail the distribution of osteoderms in this species, and the sequence of development of these elements in the body. The new data also facilitates: (b) the description of the morphological variation of individual osteoderms *in situ*. Finally, we: (c) compare the proportion of the extracranial endolymphatic sacs in the species *G. gecko* with those of other species with and without osteoderms in order to determine whether these additional ossifications are correlated with the size of these calcium-rich structures.

2 | MATERIALS AND METHODS

2.1 | Imaging techniques

We used two methods to study bony elements: digital X-rays and HRCT. Digital X-rays were taken at the Division of Amphibians and Reptiles and Ichthyology X-ray facility at the Museum Support Center of the National Museum of Natural History, Smithsonian Institution. We used an X-ray system with a KevexTM PXS10-16 W X-ray source and Varian Amorphous Silicon Digital X-Ray Detector PaxScanH 4030R set to 130 kV at 81 mA. For each X-ray, linear and pseudofilm filters were used. The HRCT scans were obtained at the University of Texas HRXCT Facility (UTCT) using a FeinFocus Microfocal source NSI scanner (Garbsen, Germany), operating at variable kV and mA values, with no X-ray prefilter. Three specimens were scanned simultaneously using a helical continued CT Scan. Volume renderings were obtained using Avizo Lite version 2019.2 (Thermo Fisher Scientific, 2019). TIFF-images from 3D-renderings were used herein for descriptions and comparisons. In addition, the individual X-rays of the premaxillary-nasal suture, fronto-nasal suture, fronto-parietal suture, and the cervical region were used for a more detailed assessment of the morphology and development of the osteoderms in different regions of the skull. A web-deliverable version of the resulting visualizations is available at Morphosource.

2.2 | Specimen source

Specimens from the group of Indopacific geckos were obtained from preserved formalin-fixed, ethanol-preserved museum specimens (Table S1). We concentrated our sampling on the genus *Gekko* as recently revised (Wood et al., 2019) and included representatives from five of the seven *Gekko* subgenera proposed, in addition to some closely related genera, *Lepidodactylus* and *Luperosaurus*. We examined a total of 100 specimens, covering 38 species. The species *G. gecko* was represented by 18 specimens, seven of which were CT-scanned and 11 were X-rayed. The specimens span a range of body sizes, with snout-vent lengths (SVL) from 42.3 to 176.7 mm. These specimens of *G. gecko* were used here as a proxy for the different stages of development, as a means to assess osteoderm development throughout ontogeny (Table 1). The SVLs, skull-lengths (SL), and extracranial endolymphatic areas were measured from X-rays in ImageJ v1.8.0 (Rasband, 2018). Sex was indicated where possible for specimens examined in this study. For many specimens, this information was available from online museum databases. Where it was not available, we determined sex of males by presence of cloacal bones (*Carphodactylidae*, *Diplodactylidae*, *Eublepharidae*, *Gekkonidae*, and *Phyllodactylidae*; following the review by Russell, Vickaryous, and Bauer (2016), or hemibacula in *Aristelliger* (*Sphaerodactylidae*), and/or females by the presence of eggs (gravid *Sphaerodactylidae* and other families).

For HRCT-scanned specimens of *G. gecko*, we calculated the same measurements, as well as osteoderm volumes using the measuring tool in Avizo. To estimate the volume of the osteoderms, these elements were segmented in Avizo and the number of voxels occupied was used as a measure of volume; volume values were regressed against SVLs to determine changes in volume with body size. For the endolymphatic area analysis, we initially followed the same approach as Lamb et al. (2017) to compare the area of the endolymphatic sacs in geckos in relation to SVL. We assessed the disparity of endolymphatic sac area among 164 samples across 113 gecko species with and without osteoderms (Table S2) using phylogenetic generalized

TABLE 1 List of *Gekko* spp. specimens discussed in this study that were scanned using high-resolution computed tomography (HRCT), including snout-vent lengths (SVL), skull lengths (SL), the region of the body that osteoderms were observed (x), and the total volume of osteoderms

Specimen number	SVL (mm)	SL (mm)	Osteoderms							Volume of osteoderms (mm ³)
			Nasals	Frontal	Parietal	Nape	Jaw	Gular	Postcranial	
<i>Gekko gecko</i>										
FMNH 261847 (♀)	61.7	19.1	–	–	–	–	–	–	x	1.7E-02
FMNH 261849 (♀)	98.8	27.3	–	x	x	x	–	–	x	31.3
FMNH 258696 (♀)	102.0	29.0	–	x	x	x	–	–	x	67.4
FMNH 266245 (♂)	113.4	31.6	–	x	x	x	–	–	x	108.2
YPM HERR 010083 (♂)	138.0	34.8	x	x	x	x	x	x	x	531.9
FMNH 236071 (♂)	143.3	38.0	x	x	x	x	–	–	x	387.2
SHSVMH-0001-2014 (♂)	167.0	46.1	x	x	x	x	x	x	x	884.0
<i>Gekko reevesii</i>										
YPM HERR 016062 (♀)	131.4	34.9	–	x	x	x	–	x	x	61.9

least squares analysis (PGLS; Grafen, 1989; Martins & Hansen, 1997; Symonds & Blomberg, 2014) and a multilocus, ultrametric phylogeny. For the phylogenetic analysis, sequences of the 16S, ACM4, CMOS, ND2, PDC, RAG-1, and RAG-2 genes were downloaded from GenBank (<https://www.ncbi.nlm.nih.gov/genbank>) for all available species with accompanying endolymphatic sac measurements (Table S3). Sequences were aligned using MAFFT v7.429 (Katoh & Standley, 2013), and a partitioning and model scheme identified using PartitionFinder v2.1 (Lanfear, Frandsen, Wright, Senfeld, & Calcott, 2016), considering all genes and codon positions as potentially different partitions. The best-fitting partitioning scheme and models were used to produce a maximum likelihood (ML) tree estimate in IQ-TREE v1.5 (Nguyen, Schmidt, von Haeseler, & Minh, 2015). A preliminary ultrametric tree was then estimated under Penalized Likelihood in the package "ape" v5.3 (Paradis & Schliep, 2018) in R v3.5.1 (<http://www.R-project.org>; R Core Team, 2012), which was then used as a starting tree for a finalized ultrametric phylogeny estimated in BEAST v1.10.4 (Suchard et al., 2018). The BEAST analysis used the same partitions as

the ML analysis and was implemented as four parallel runs of 100 million generations, sampling every 10,000 generations. The first 15 million generations of each run were discarded as burn-in, with the final consensus tree generated from the combined output of the four runs (Figure S1). When more than one individual was measured per species, we used the largest specimen in the analysis. Comparative analyses were conducted in R with the packages "geiger" v2.0.6.2 (Harmon, Weir, Brock, Glor, & Challenger, 2008) and "ape."

3 | RESULTS

3.1 | Occurrence of osteoderms

Cephalic osteoderms were only found in large specimens of the species *G. gecko*, and in one specimen assignable to *G. reevesii* GRAY 1831 (Table 1). The minimum sized individual in which we detected the presence of osteoderms was a *G. gecko* of 98.8 mm SVL. Of the

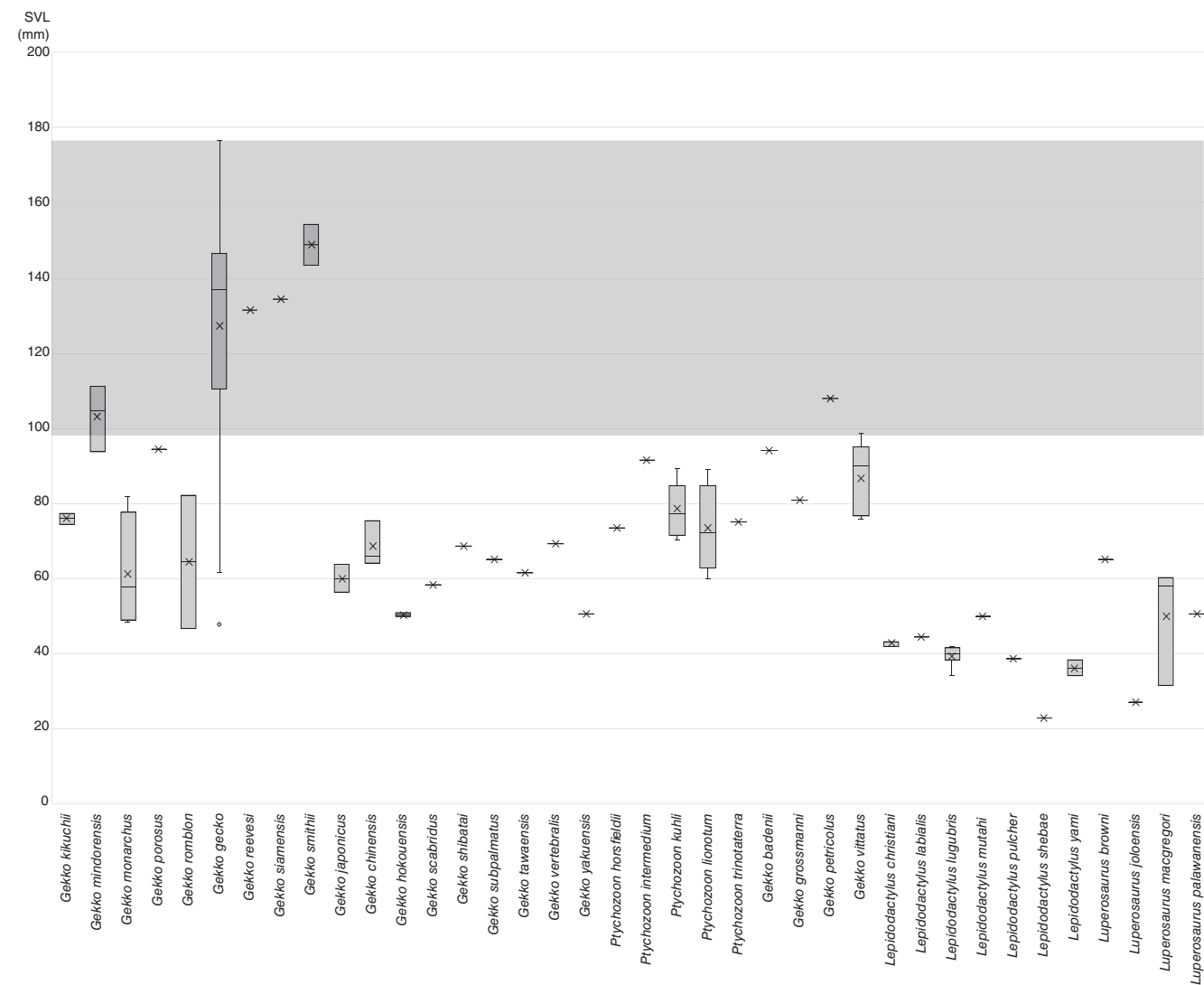


FIGURE 1 Box plot of the snout-vent length (SVL) in mm of specimens sampled. Gray area indicates the size range where osteoderms were detected in species of the genus *G. gecko* and *G. reevesii*. Note that only a few species were represented by specimens within this range

38 species examined, only five additional species exceed this minimum SVL—*Gekko mindorensis* TAYLOR 1919, *G. petricolus* TAYLOR 1962, *G. reevesii*, *G. siamensis* GROSSMANN & ULMER 1990, and *G. smithii* GRAY 1842—yet osteoderms were not detected in any of our HRCT or X-ray scans from these specimens either (Table S1). These new data suggest that the presence of osteoderms in the group of Indopacific geckos occurs only in large specimens of large species (i.e., at least 98.8 mm SVL; *G. gecko*, *G. reevesii*), as the majority of the specimens sampled where no osteoderms were found were <98.8 mm in SVL (Figure 1). The maximum sized individual of *G. gecko* we measured in this work was from Burma and had an SVL of 176.7 mm (USNM 564836; Figure 2), approaching the largest reported values for this species, 176.0–178.0 mm (Bauer, 2013; Russell & Bauer, 1987).

3.2 | Pattern of development of osteoderms in *Gekko gecko*

The smallest HRCT specimen (SVL 61.7 mm, SL 19.1 mm, FMNH 261847, ♀) shows characteristics of immature specimens, such as paired parietals and nasals (Daza et al., 2015); partially ossified

pectoral girdle, pelvic girdle, and tarsal elements; and nonossified carpal, and epiphyses of long bones. Osteoderms were not present within this specimen (Figures 3a, 4a, and 5a).

Osteoderms were visible in slightly larger HRCT (and X-ray) specimens (Figures 3 and 6). Onset of osteoderm development occurred at the same size range in both males and females of *G. gecko*, and there was no obvious sexual dimorphism in osteoderm volume or distribution. Sexual dimorphism in this species in general has also been noted to be minimal (Fitch, 1981). To simplify the description of the osteoderm development, we describe the distribution of osteoderms

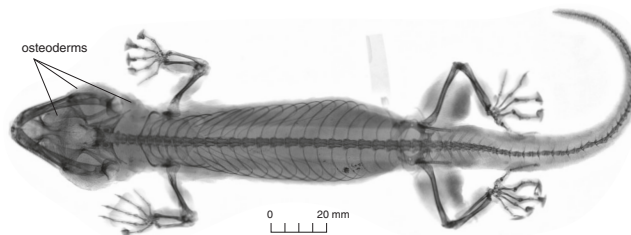


FIGURE 2 *Gekko gecko*, digital X-ray of the largest specimen included in this study (Snout-vent length [SVL] 176.7 mm, USNM 564836 [♀])

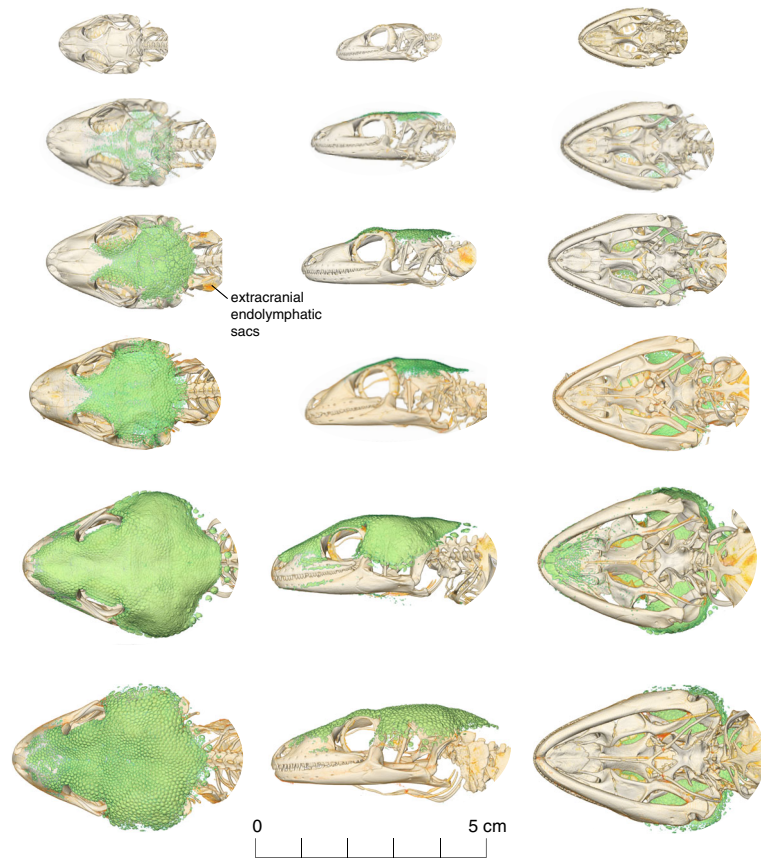
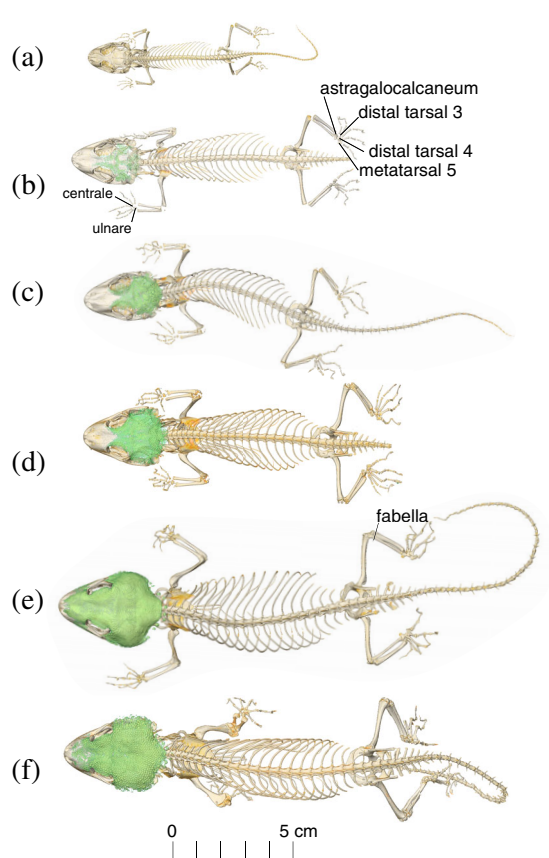


FIGURE 3 *Gekko gecko*, osteoderm growth trajectory and volume in specimens observed using high-resolution computed tomography (HRCT). Specimens: (a) FMNH 261847 (♀), (b) FMNH 261849 (♀), (c) FMNH 258696 (♀), (d) FMNH 266245 (♂), (e) YPM HERR 010083 (♂), and (f) FMNH 236071 (♂), are displayed in a developmental progression from smallest (a) to largest (f). The osteoderms are rendered in green to distinguish them from the rest of the skeleton

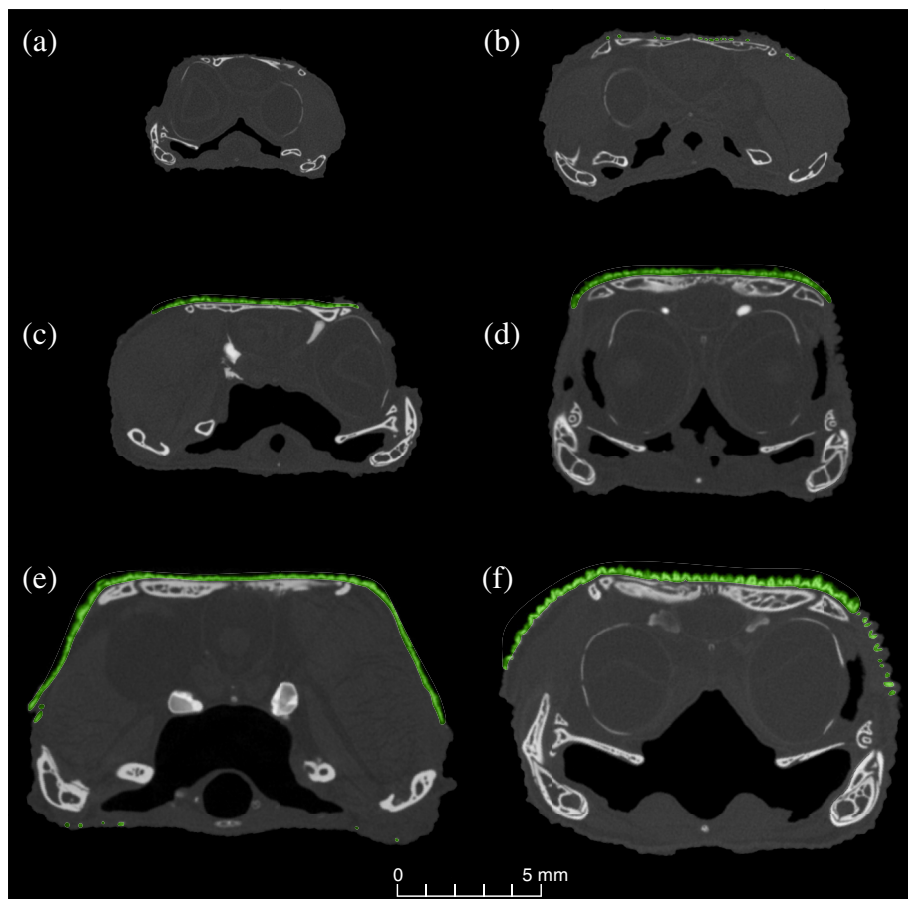


FIGURE 4 *Gekko gecko*, transverse cross-section tomogram at the level of the frontoparietal suture of the specimens: (a) FMNH 261847 (♀), (b) FMNH 261849 (♀), (c) FMNH 258696 (♀), (d) FMNH 266245 (♂), (e) YPM HERR 010083 (♂), and (f) FMNH 236071 (♂)

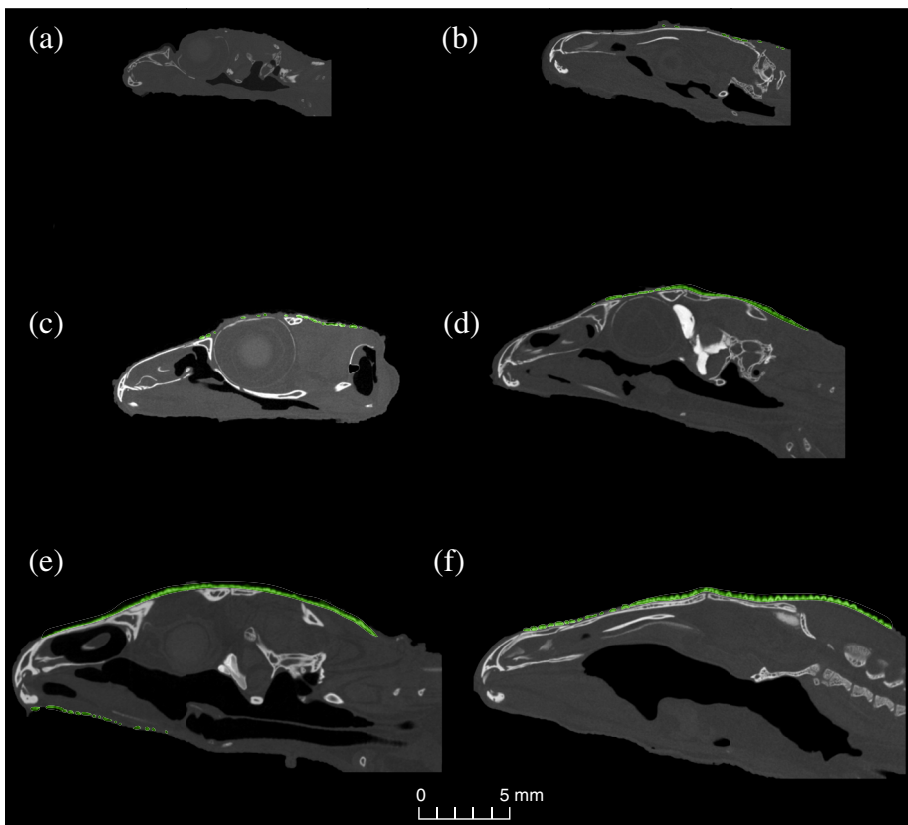


FIGURE 5 *Gekko gecko*, midsagittal cross-section tomogram of the specimens: (a) FMNH 261847 (♀), (b) FMNH 261849 (♀), (c) FMNH 258696 (♀), (d) FMNH 266245 (♂), (e) YPM HERR 010083 (♂), and (f) FMNH 236071 (♂)

for each specimen ordered by increasing size, followed by a brief comment on visible changes to the skeleton.

SVL 98.8 mm, SL 27.3 mm (FMNH 261849, ♀, Figures 3b, 4b, and 5b). The osteoderms in this specimen appear as scattered condensations overlying the prefrontal, orbits, frontal, parietal, squamosal, supraoccipital, and on top of the temporal region; yet there are still several spaces free of osteoderms. The osteoderms extend posteriorly to the level of the atlas. Individual osteoderms are ring-shaped with a void space in the center (Figure 3b).

The nasals and parietals have started to fuse together and although epiphyses and metaphyses are still cartilaginous, they are starting to show some of the carpal, tarsal, and elbow and knee sesamoid elements. The wrist of the specimen shows two bones, the ulnare (proximal to the ulna) and the centrale, located in the middle of the wrist (Figure 3b). In the elbow and knee joints, there are epiphyseal ossification centers, and in the ankle, there are four elements: the astragalocalcaneum, two distal tarsals (3 and 4), and the metatarsal V (Figure 3b).

SVL 102.0 mm, SL 29.0 mm (FMNH 258696, ♀, Figures 3c, 4c, and 5c). Despite the similar body size between this specimen and the previous one, there are striking differences between them in both osteoderm volume and ossification. In this specimen, the osteoderms are more densely packed, forming a continuous armor that covers the same bones, in addition to the postorbitofrontal. The osteoderms cover the entire surface of these bones with no exposure of the surface except for the anterior portion of the frontal, which remains exposed. The cephalic shield covers the orbits (eyes) more extensively and descends laterally and extends posteriorly to cover the level of the third cervical vertebra.

The nasals and parietals still show ongoing fusion (Daza et al., 2015), the epiphyses and metaphyses are still cartilaginous, showing two bones in the wrist (ulnare and centrale). The elbow and knee joints show additional ossification centers and epiphyses, and in the ankle the same four elements are observed as in the previous specimen.

SVL 113.4 mm, SL 31.6 mm (FMNH 266245, ♂, Figures 3d, 4d, and 5d). At this size, the specimen shows additional concentration of osteoderms on top of the temporal area and the entire surface of the postorbitofrontal, following a neat pattern around the orbit. The osteoderms form a continuous structure similar to a helmet, completely covering the mandibular fossa when viewed in dorsal view and overlying the entirety of the squamosal. The layer of osteoderms appears to be denser than in smaller specimens. Some of the individual osteoderms still have a void space in the center.

The epiphyses and metaphyses still show signs of being cartilaginous, but they display an increasing number of ossification centers near the long bones in the elbow (5), wrist (4), and knee (~4). Major changes in the ankle are concentrated on the epiphyses of the tibia and fibula.

SVL 138.0 mm, SL 34.8 mm (YPM HERR 010083, ♂, Figures 3e, 4e, and 5e). The osteoderms in this stage also cover the snout, including the entire frontal, nasals, prefrontal, and a large portion of the facial process of the maxilla, and some independent patches additionally cover the side of the posterior process of the maxilla. The osteoderms reach the limit between the premaxilla and the nasals. On the lateral side, the osteoderms extend more laterally covering the entire temporal region (including the entire lateral side, and forming a bony shield behind the orbit), and even reaching the eminence of the

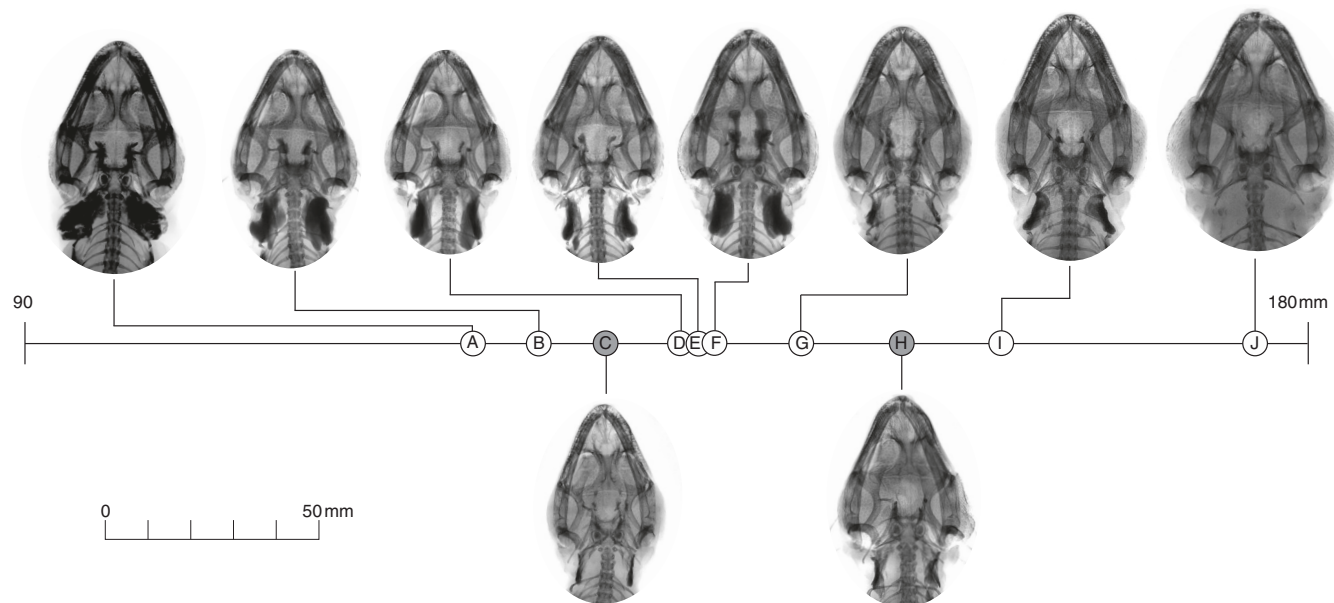


FIGURE 6 *Gekko gecko*, osteoderm growth trajectory and volume in specimens observed using digital X-rays. Numbers in parentheses after specimen numbers are snout-vent lengths (SVLs) in mm: (a) USNM 318728 (122.2, ♀), (b) USNM 512854 (126.4, ♀), (c) USNM 564835 (131.5, ♂), (d) USNM 512855 (136.6, ♀), (e) USNM 512857 (137.5, ♀), (f) USNM 573671 (138.3, ♀), (g) USNM 564838 (144.9, ♀), (h) USNM 512856 (152.3, ♂), (i) USNM 564837 (158.7, ♀), (j) USNM 564836 (176.7, ♀)

coronoid. Osteoderms are also present on the lateral side of the jaw, partially covering the dentary, and a large patch is present on the mental and chin area. The osteoderm shield extends posteriorly to the level of the fifth cervical vertebra, where there is an isolated row of large conical osteoderms.

The epiphyseal plate and ossification centers are entirely fused, indicating skeletal maturity (Maisano, 2002). The elbow, wrist, knee, and ankle joints are also completely ossified. There is a sesamoid on the proximal side of the radius, and the fabella sesamoid is observed on the posterior side of both knees.

SVL 143.3 mm, SL 38.0 mm (FMNH 236071, ♂, Figures 3f, 4f, and 5f). Although this specimen is slightly larger than the previous one (YPM HERR 010083), it shows a lower volume of osteoderms. It has a similar distribution of osteoderms to the previous specimen but does not have osteoderms in the lower jaw region. The snout is also extensively covered by osteoderms, although these elements are scattered over the top of the nasals and the nasal-premaxilla suture.

The osteoderm distribution on the dorsal part of the skull in this specimen is similar to that of specimen YPM HERR 010083, except that the snout retains some spaces without osteoderms. In addition,

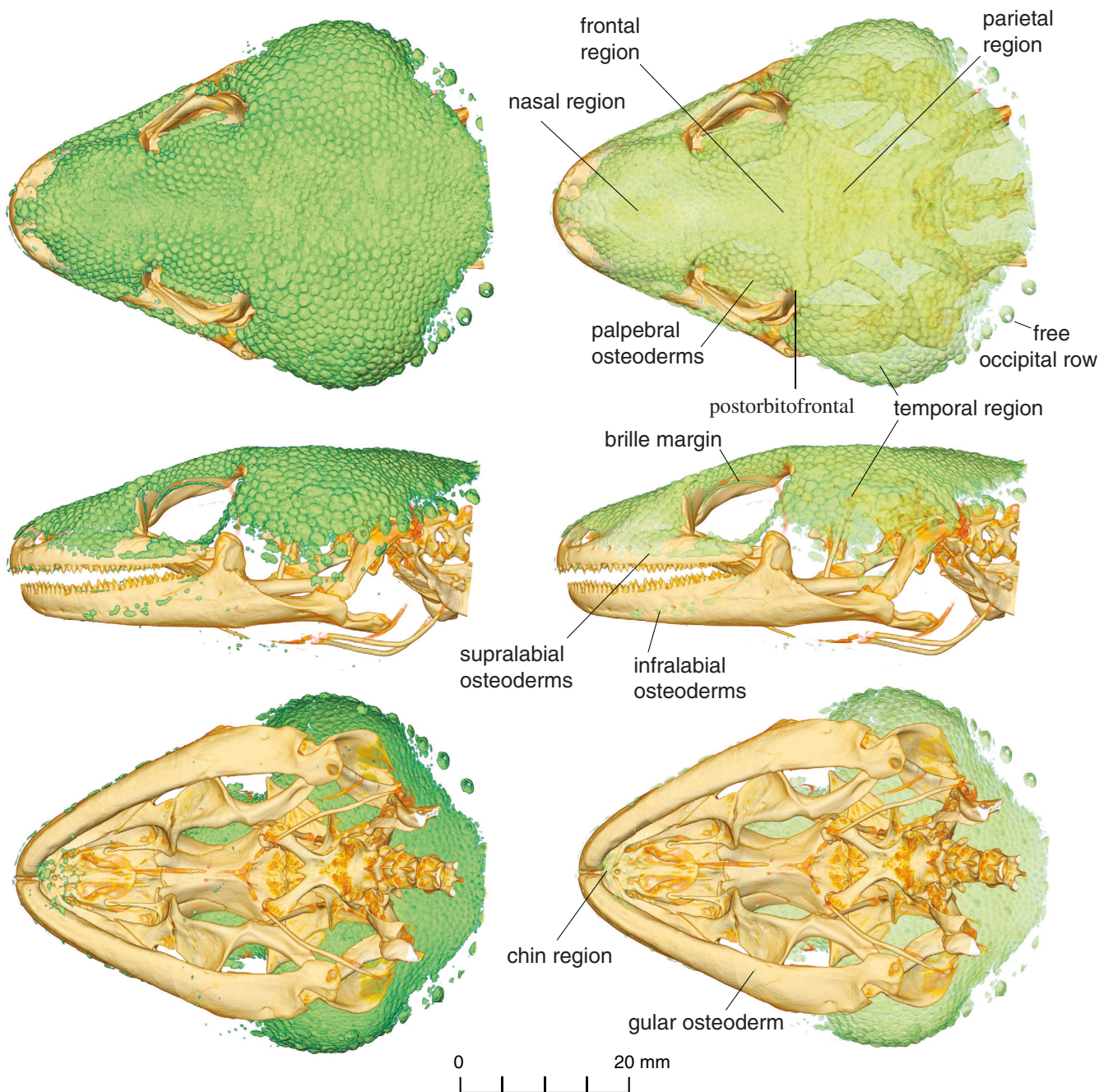


FIGURE 7 *Gekko gecko*, details of the osteoderms of the largest high-resolution computed tomography (HRCT) specimen (SHSVMH-0001-2014, ♂) showing individual variation of the osteoderms at different regions of the skull

specimen FMNH 236071 has osteoderms on the tip of the facial process of the maxilla and only a small spot on the posterior part of this process. Although FMNH 236071 is larger than YPM HERR 010083, the former does not exhibit osteoderms in the gular region.

SVL 167.0 mm, SL 46.1 mm (SHSVMH-0001-2014, ♂, Figure 7). Specimen SHSVMH-0001-2014 was illustrated previously (Daza et al., 2015); we have here produced images in all views to better illustrate the position of the osteoderms. We also use this specimen to describe the individual variation of osteoderms in this species. The osteoderms in this specimen cover virtually the entire surface of the cranium and portions of the jaw; the ascending nasal process of the premaxilla is covered, leaving only the labial margin of the maxilla exposed.

Individual osteoderm variation of the cephalic osteoderms: In specimen SHSVMH-0001-2014, the differentiation in the osteoderms is more marked, both in size and shape; osteoderms vary in size

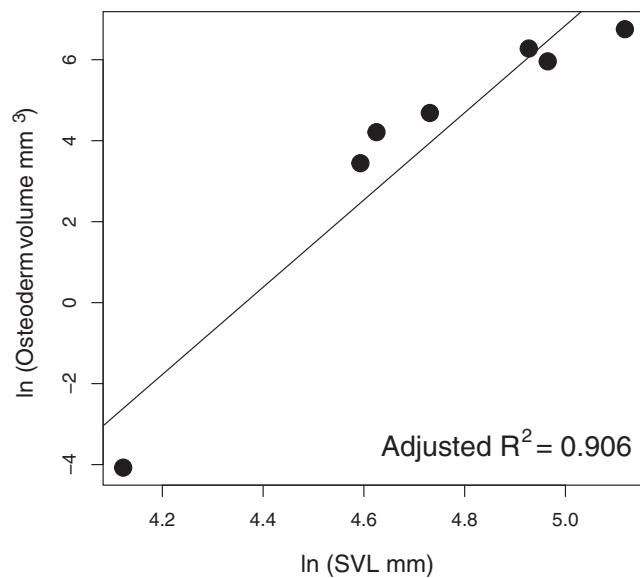


FIGURE 8 Increase in osteoderm volume in *Gekko gecko* along a body-size gradient, with data from samples presented in Figure 3. Log-transformed snout-vent length (SVL) in mm, log-transformed osteoderm volume measured in cubic mm

depending on the area of the head or body where they are formed. The smallest osteoderms are those along the midrow of the skull from the nasal region to anterior portion of the parietals, the ones forming the chin patch and the ones scattered on the gular region. The largest osteoderms are located in the temporal region, and they enlarge as they approach the posterior border, especially the ones forming the free occipital row. Some of the largest osteoderms still preserve the void space in the middle (e.g., those of the occipital row). Osteoderms are arranged in an interlocking pattern similar to puzzle pieces, and the majority are either tubercular or doughnut shaped. The osteoderms associated with the supralabial and infralabial scales tend to be more irregular and elongated, almost rectangular. There is a line of slim and elongated osteoderms surrounding the upper margins of the brille (Figure 7).

We observed that in *G. gecko*, osteoderm volume increases linearly along the body size gradient (Figure 8), and the relationship between size and volume shows positive allometry, as defined by the equation with an allometric coefficient higher than 10 ($y = 10.777x - 20.428$). This data indicates that osteoderm volume increases rapidly with respect to body length (SVL), which is consistent with the pattern described. Once the osteoderms overlay certain areas of the skull (i.e., frontal, parietals) the individual dermal structures begin to expand and fill the space between them and within their central void spaces.

3.3 | Osteoderms in *Gekko reevesii*

One of the specimens studied (YPM HERR 016062, ♀, SVL 131.4 mm, SL 34.9 mm, Figure 9) was assignable to the species *Gekko reevesii* from southern China, representing a second species where these structures are found. The pattern of osteoderm distribution in this species is different to the one seen in the series of *G. gecko*. The osteoderms in this specimen, which has a skull length comparable with YPM HERR 010083, appear to present a less dense layer. Contrary to YPM HERR 010083, osteoderm distribution is similar to the skeletally immature specimens of *G. gecko* (e.g., FMNH 261849), although the osteoderms are more concentrated on the palpebral

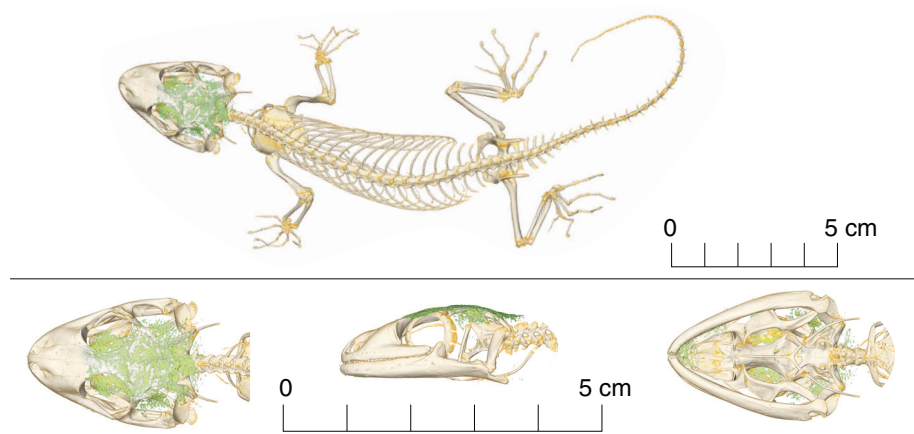


FIGURE 9 *Gekko reevesii*, details of the osteoderms of the High-Resolution Computed Tomography scan (specimen: YPM HERR 016062, ♀). The osteoderms are rendered in green to distinguish them from the rest of the skeleton

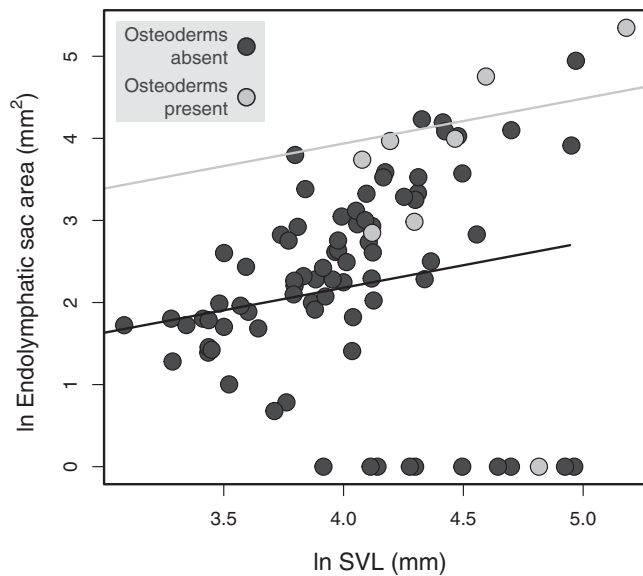


FIGURE 10 Plot of log-transformed endolymphatic sac area (mm^2) against $\log(x + 1)$ -transformed snout-vent length (SVL, mm), with fitted lines from a phylogenetic generalized least squares (PGLS) model that includes the presence/absence of osteoderms as treatment. Gecko species with osteoderms tend to have larger endolymphatic sac area, and similar slopes with different intercepts are consistent with different phenotypic optima

region, and are very scattered on top of the frontal, postorbitofrontal, parietal, supraoccipital, and the temporal region. One major difference is that despite the lower volume of osteoderms compared with *G. gecko* of similar size, this species displays osteoderms in the chin area, which tend to be developed in much later stages in *G. gecko*.

3.4 | Do endolymphatic sac proportions vary with presence of osteoderms?

Gecko species with osteoderms have larger endolymphatic sacs than gecko species without osteoderms, taking into account SVL (Figure 10). PGLS results support that the models for endolymphatic sac area of geckos with or without osteoderms have similar slopes but the slopes have different intercepts. The PGLS model with osteoderms as treatment (endolymphatic sac area $\sim \ln[\text{SVL}] + \text{osteoderms}$) received moderately stronger support than the model without treatment (endolymphatic sac area $\sim \ln[\text{SVL}]$, $\Delta\text{AIC} = 7.13$). These findings imply that the extracranial endolymphatic sacs tend to be larger in gecko species with osteoderms than in species without osteoderms.

4 | DISCUSSION

4.1 | Onset of osteoderm development

Previously, osteoderms were considered to be absent from the hatching stage (SVL < 80.0 mm) to less than 111.5 mm SVL, which was the

stage at which the first appearance of osteoderms was noted in *G. gecko* (Vickaryous et al., 2015). In our sampling, we noticed the presence of osteoderms in even smaller specimens (98.8 mm SVL). It is clear that these structures develop before the onset of skeletal maturity.

In both *Gekko* species where the presence of osteoderms was observed, the timing of appearance of these elements (based on comparison of similar sized specimens) is asynchronous to previous reports (Vickaryous et al., 2015). The development of osteoderms in *G. gecko* can be described in three main stages: (a) In skeletally immature specimens, osteoderms appear overlying the posterior portion of the frontal bone, palpebral region, parietals, supraoccipital, and the temporal region (Figures 3b-d, 4b-d, and 5b-d). (b) In young adults, the osteoderms extend further toward the snout region, entirely covering the frontal bone, nasals, premaxilla, maxilla, and prefrontal (Figures 3f, 4f, and 5f). (c) In the last stage, specimens are skeletally mature and develop osteoderms covering the entire dorsal surface of the cranium and extending to the labial side of the jaw and chin areas (Figures 3e, 4e, 5e, and 7). In the second and third stages, there is a noticeable incremental increase in osteoderm volume, to the point where spaces between individual elements are filled out.

Previously, it was described that individuals around the SVL of 111.5 mm (comparable to the first stage) have osteoderms restricted to the frontal bone and orbits, and no postcranial osteoderms (Vickaryous et al., 2015). We found here that osteoderms also covered the parietals, postorbitofrontals, supraoccipital, and the temporal region. It is possible that the HRCT-method better reveals the more posterior osteoderms compared to clear and staining. Our results are congruent with the Vickaryous et al. (2015) study where they further report the appearance of osteoderms covering most of the head (except the rostral-most tip) in slightly larger individuals (SVL 116.2 mm), and found no evidence of osteoderms beneath the supralabial scales, and only some mineralization subadjacent to the infralabials and across the gular region, and in the tubercles dorsal to the pectoral girdle. Vickaryous et al. (2015) described that in specimens larger than 121.9 mm SVL (equivalent to the second stage), most, if not all, of the dorsal surface of the head (excluding the supralabial scales) is completely reinforced with osteoderms, including the gular region, and within dermal stroma of the tubercular scales across the trunk and limbs. Postcranial osteoderms in the trunk or limbs were not as evident as cephalic osteoderms in the full body HRCT-datasets, and were instead observed as scarcely and randomly distributed, small and irregularly shaped osteoderms, most similar in form to those seen in the gular region. These few osteoderms were observed infrequently scattered in both dorsal and ventral surfaces of the trunk and limbs in all specimens, including the juvenile specimen which showed no cranial osteoderms (FMNH 261847, see Table 1), but were so small that most do not display in the HRCT volume renderings, in contrast to the cranial osteoderms. These discrepancies between this study and that of Vickaryous et al. (2015) may be attributed to the resolution of the scans and the size of these structures.

The species *G. reevesii* is the sister species of *G. gecko* and the two species were long considered to be conspecific (Rösler et al.,

2011). Based on the single available specimen of this species, it appears that the osteoderms may develop in a slightly different pattern to those in *G. gecko*, similar to observations of variation in timing and patterns of osteoderm accumulation in different species of *Tarentola* (Vickaryous et al., 2015). The specimen of *G. reevesii* studied measured 131.4 mm SVL; considering that this species attains a maximum of at least 173.0 mm SVL (Rösler et al., 2011), and the degree of ossification of the epiphyses and joint elements, we estimate this specimen to be a young adult. However, it already displays osteoderms in the chin region, prior to an increase in the osteoderm volume, and to development of these elements over the snout and jaw. A more detailed study of *G. reevesii*, including more specimens, is needed to corroborate this asynchronous ossification pattern. At this point, we cannot conclude whether this species develops similar volume of osteoderms in the skull as *G. gecko*. Likewise, we lack complete data on osteoderm development for other extremely large species of the subgenus *Gecko* (e.g., *G. albofasciolatus* GÜNTHER 1867, *G. nutaphandi* BAUER, SUMONTA, & PAUWELS 2008, *G. verreauxi* TYTLER 1865), and for some species we are lacking specimens near the maximum size limit (e.g., *G. smithii*; Rösler et al., 2011); although none of the three adult specimens of *G. siamensis* or *G. smithii* included in this study have osteoderms. It would seem that large size may facilitate the appearance of the cephalic osteoderms in the genus *Gekko*; an analogous association between large size and the occurrence of parafrontal bones was reported in the Old World radiation of sphaerodactylid geckos (Griffing, Daza, DeBoer, & Bauer, 2018).

4.2 | Comments on the distribution and functionality of osteoderms in geckos

Among the three gekkotan genera that exhibit osteoderms, different patterns of osteoderm distribution are observed. In terms of body coverage, osteoderms in *Geckolepis* (Gekkonidae) superficially resemble the body armor developed in skinks, where the whole body is covered by large, overlapping cycloid scales (except in the chin area); although the microstructure of the osteoderms in *Geckolepis* differ substantially from skinks in that they are much thinner, more pliable, and also ephemeral structures that are easily shed during regional integumentary loss (Paluh et al., 2017). The genus *Tarentola* (Phyllodactylidae) has been shown to exhibit osteoderms in multiple species (*T. americana* GRAY 1831, *T. annularis* GEOFFROY SAINT-HILAIRE 1827, *T. chazaliae* MOCQUAD 1895, *T. crombiei* DIAZ & HEDGES 2008, *T. mauritanica* LINNAEUS 1758, *T. neglecta* STRAUCH 1887; Levrat-Calviac, 1986; Levrat-Calviac & Zylberberg, 1986; Vickaryous et al., 2015), representative of all four subgeneric clades within this genus (Carranza, Arnold, Mateo, & Geniez, 2002; Carranza, Arnold, Mateo, & López-Jurado, 2000). Different species studied across *Tarentola* have been shown to display differential degrees of osteoderm development, however, these structures are still more permanent than in *Geckolepis* and are developed in the cranial and postcranial regions (Vickaryous et al., 2015). The osteoderms of *Tarentola*

are more dense around the skull, and may overly the lower jaw and the chin region (Vickaryous et al., 2015). When these structures are developed in the postcranium of *Tarentola*, in cleared and stained preparations they appear as scattered structures in the dorsal region of the body (Vickaryous et al., 2015), however, they form an almost continuous layer of dermal bone comprised of thousands of tiny isolated elements (Avallone, Tizzano, Cerciello, Buglione, & Fulgione, 2018); the discrepancy in the degree of covering reported in these two studies is likely attributed to sexual, ontogenetic, and geographical differences. Osteoderms in the genus *Gekko* (Gekkonidae) are more similar to those of *Tarentola* spp. and other squamates in terms of permanency and morphology (juxtaposed, polygonal; Parker & Taylor, 1942).

A diversity of functions have been proposed for osteoderms including roles in protection (Broeckhoven et al., 2017; Moss, 1969; Vickaryous et al., 2015), locomotion (Buchwitz et al., 2012; Buchwitz & Voigt, 2010; Dilkes & Brown, 2007; Frey, 1988; Seidel, 1979), calcium mineral storage (Curry Rogers et al., 2011; Dacke et al., 2015; Klein, Scheyer, & Tütken, 2009), and thermoregulation (Farlow et al., 1976; Farlow et al., 2010; Seidel, 1979), or a combination of these functions (Broeckhoven et al., 2017). For example, Broeckhoven et al. (2017) provided evidence for a functional trade-off between strength and thermal capacity of osteoderms in two species of girdled lizards.

Considering reinforcement of the integument, a body armor covering can not only serve as an antipredator defense but can also act to prevent intraspecific aggression, as well as protect against dangerous prey commonly encountered by some of the armored gecko species (Vickaryous & Sire, 2009). *Geckolepis* osteoderms have been inferred to function more as thermoregulation structures or deposits of labile calcium for eggshell formation (Paluh et al., 2017). On the other hand, extreme shedding, such as observed in *Geckolepis* (Paluh et al., 2017; Schmidt, 1911, 1912), could be also interpreted as an antipredator strategy that might trick the hunter; shedding a large amount of hardened integument could work in a similar way to other antipredator strategies, such as tail autotomy, which is a widespread strategy among squamates (Hofstetter & Gasc, 1969; McConnachie & Whiting, 2003), being developed in 13 families (Stanley et al., 2019). The protective nature of osteoderms is consistent with large specimens of *G. gecko* being capable of preying upon vertebrates, in addition to invertebrates, that have the potential to injure their heads (e.g., birds, geckos, rodents, and snakes; Bucol & Alcala, 2013; and see review in Daza, Herrera, Thomas, & Claudio, 2009). Furthermore, to kill large prey items *G. gecko* is known to exhibit the peculiar behavior of smashing their heads and the prey against the substrate, hence the cephalic shield may offer additional protection (Bucol & Alcala, 2013). In cordylid lizards, osteoderms increase skin toughness, serving as an antipredator strategy by withstanding bite forces of mammalian predators; however, predation by snakes and thermoregulation might cause variation in defensive morphology (Broeckhoven et al., 2015). A similar conclusion can be drawn for the species *G. gecko*, as they are also preyed upon by snakes (e.g., Golden tree snake, *Chrysopelea ornata*—Shaw, 1802; Babu, Shihan, Debbarma, & Debbarma, 2018).

The pattern of osteoderm distribution in *G. gecko*, limited to the head with scattered small elements on the dorsal side of the trunk, argues against any physiological role (thermoregulation, water loss), and to some extent protection against some predators/prey, although some protection might be offered against direct strikes to the head by conspecifics or prey. Males of *G. gecko* are known for being territorial and aggressive (Henkel & Schmidt, 1995; Marcellini, 1977; Seufer, 1991), especially when defending their eggs and offspring (Petzold, 2007). In *G. gecko*, restriction of the osteoderm layer to predominantly form a cephalic shield over the dorsal surface of the head could relate to such agonistic behaviors (Vickaryous et al., 2015). The osteoderm distribution pattern in *G. gecko* differs considerably from the pattern seen in heavily armored lizards (e.g., cordylids and gerrhosaurids), which in fact display a wide range of different combinations of areas covered (Stanley, 2013), including: (a) full-body covering (e.g., *Broadleysaurus major* DUMÉRIL 1851, *Ouroborus cataphractus* BOIE 1828, *Smaug giganteus* SMITH 1844), (b) head, limbs, and tail covered (e.g., *Pseudocordylus transvaalensis* FITZSIMONS 1943), and (c) body covering reduced or absent and tail covered (e.g., *Platysaurus ocellatus* BROADLEY 1962). Tail cover is important for cordylids and gerrhosaurids considering that some of them use crevices as retreats, oftentimes leaving the tail exposed. In the case of geckos, where the tail is commonly shed, development of caudal osteoderms seems certainly ineffective since it would be a wasted investment of energy and calcium; nevertheless, they can be present in the tail (e.g., in *Tarentola*).

The idea that these dermal structures might work as additional deposits of calcium has been proposed (Paluh et al., 2017), and could be similar to how alligators may source calcium from osteoderms for eggshell production (Dacke et al., 2015). Alternatively, calcareous materials are produced in the endolymphatic apparatus of all vertebrates (Whiteside, 1922), and in some geckos and iguanians the endolymphatic sacs become greatly enlarged, forming protruding structures extracranially (Kluge, 1967). These structures are found mainly in the neck and sometimes anterior to the braincase, which extend via a foramen that opens from the anterior semicircular canal (pathway of the accessory endolymphatic duct, Conrad & Daza, 2015). It seems plausible that, at least in geckos and iguanians, the endolymphatic sacs are supplying all the calcium necessary for egg production (Bauer, 1989; Kluge, 1967; Lamb et al., 2017). In the sphaerodactylid gecko *Gonatodes antillensis* LIDTH DE JEUDE 1887 it has been shown that females develop larger endolymphatic sacs than males, and that gravid females have slightly larger endolymphatic sacs than nongravid females (Lamb et al., 2017). Kluge (1967) illustrated an adult male and female specimen of *G. gecko*, highlighting that males lack extracranial endolymphatic sacs, while in females these structures appear very enlarged. In our sampling, we found that these sacs were also present in males, but frequently are smaller than in females (Figure 6, Table S2).

Considering the results of the analysis of endolymphatic sac areas as an approximation of the size of these structures, it seems that for its size, *Gekko gecko*, along with other gecko species with osteoderms, has proportionally larger endolymphatic sacs compared to geckos

without osteoderms (Figure 10). Given the rare occurrence of osteoderms across gekkotans however (three small clades), even with unlimited species sampling it may remain impossible to draw strong conclusions about the relationship between endolymphatic sac size and osteoderms. Furthermore, size of endolymphatic sacs is highly variable among geckos, including differences among species or families (e.g., sacs tend to be absent in diplodactylids, likely because this family lay leathery rather than hard-shelled eggs), between sexes, stage of reproductive cycle in females, and availability of calcium in diet (e.g., captive animals). Given this variability and that our sampling only included a few individuals per species, we recommend considering this a preliminary analysis and interpreting these results with caution until more accurate approaches are applied to study these structures in depth (e.g., diffusible iodine-based contrast-enhanced computed tomography [DiceCT], detailed dissections, vital staining of the calcium, or postmortem staining of large sample sizes for many species). Despite the limitations of these data, our analysis suggests that in geckos with osteoderms, the endolymphatic sacs might have a dual function as a source of calcium, not only for egg production, but also for the extra bone material. We propose that osteoderms represent structures that require rather than provide calcium resources and would predict that if the opposite were the case, the endolymphatic sacs in geckos with osteoderms would be more likely to be reduced in size compared to the body size.

5 | CONCLUSIONS

Despite our broad species sampling, osteoderms were only confirmed in two sister taxa (*G. gecko* and *G. reevesii*), therefore, these dermal structures are a synapomorphy for this clade of geckos. Osteoderms in other geckos, since they occur in quite divergent clades, and due to their overall differences in permanence (*Geckolepis*), morphology (*Tarentola*), and spatial distribution (both), are independently acquired and nonhomologous.

Although these structures are homologous in the two species of the group of Indopacific geckos, we found disparity between these two species in the timing of development of the osteoderms. A more detailed assessment of the development of this trait is required in *G. reevesii*, including additional specimens of varying size, in order to better understand the developmental discordance.

In *G. gecko* and *G. reevesii*, osteoderms are likely to reinforce the integument, especially in large specimens that might be more exposed to agonistic behavior of conspecifics or large prey items, as a consequence of increase in diversity of dietary items during ontogeny. With current data, we cannot conclude if the osteoderms in *G. gecko* function as calcium reservoirs, however, our data implies that increased auxiliary structures (i.e., extracranial endolymphatic sacs) in gecko species with osteoderms possibly fulfill this function. Conclusively determining the final storage area of calcium could be done experimentally by feeding captive geckos with calcium isotopes and tracking the pathway of calcium accumulation in the body.

ACKNOWLEDGMENTS

The authors would like to acknowledge Jessie Maisano and Matt Colbert from The University of Texas High-Resolution X-ray Computed Tomography Facility for scanning all the specimens for the NSF Collaborative Research: RUI: From Exaptation to Key Innovation – Evolutionary Insights from Gliding Geckos. We thank Patrick Lewis for providing further HRCT scans; thanks to Kevin de Queiroz, Rayna Bell, Kenneth Tighe, Addison Wynn, Steve Gotte from the Division of Amphibians and Reptiles at the National Museum of Natural History, Smithsonian Institution, and Maria Camila Vallejo, Elizabeth Sullivan, and Christopher Schalk for their help obtaining digital X-rays. We also would like to thank Greg Watkins-Colwell (Yale Peabody Museum of Natural History), Lauren Scheinberg (California Academy of Sciences), and Alan Resetar (The Field Museum) for access to specimens under their care. This study was funded in-part by the National Science Foundation (DEB1657662 awarded to T.G.; DEB1657656 awarded to J.D.D.; DEB1555968 awarded to A.M.B.; DEB1657527 awarded to M.P.H.), and experiment.com.

AUTHOR CONTRIBUTIONS

J.D.D. and M.P.H. conceived of the study; R.J.L., C.H.M., K.L., M.P.H., T.G., and J.D.D. collected and analyzed data; R.J.L., C.H.M., M.P.H., T.G., and J.D.D. produced the figures; M.P.H., T.G., A.M.B., and J.D.D. contributed funding; all authors contributed to writing of the manuscript.

DATA AVAILABILITY STATEMENT

Data availability statement: The data that support the findings of this study are available from the corresponding author upon reasonable request.

ORCID

Rebecca J. Laver  <https://orcid.org/0000-0002-6319-7213>
 Cristian H. Morales  <https://orcid.org/0000-0001-9964-9173>
 Matthew P. Heinicke  <https://orcid.org/0000-0002-6021-8058>
 Tony Gamble  <https://orcid.org/0000-0002-0204-8003>
 Kristin Longoria  <https://orcid.org/0000-0003-0885-6148>
 Aaron M. Bauer  <https://orcid.org/0000-0001-6839-8025>
 Juan D. Daza  <https://orcid.org/0000-0002-5651-0240>

REFERENCES

Angel, F. (1942). Les lézards de Madagascar. *Memoires De L'academie Malgache*, 36, 1–193.

Arnold, E. N. (1989). Towards a phylogeny and biogeography of the Lacertidae: Relationships within an Old World family of lizards derived from morphology. *Bulletin of the British Museum of Natural History*, 55, 209–257.

Auffenberg, W. (1981). *The behavioral ecology of the komodo monitor*. Gainesville, FL: University Press.

Avallone, B., Tizzano, M., Cerciello, R., Buglione, M., & Fulgione, D. (2018). Gross anatomy and ultrastructure of Moorish Gecko, *Tarentola mauritanica* skin. *Tissue and Cell*, 51, 62–67. <https://doi.org/10.1016/j.tice.2018.03.002>

Babu, M. Q., Shihan, T. R., Debbarma, R., & Debbarma, P. (2018). *Chrysopelea ornata* (Ornate flying snake) diet. *Herpetological Review*, 49 (3), 544–545.

Barahona, F., & Barbadillo, L. J. (1998). Inter-and intraspecific variation in the post-natal skull of some lacertid lizards. *Journal of Zoology*, 245(4), 393–405. <https://doi.org/10.1111/j.1469-7998.1998.tb00114.x>

Batista, A., Hertz, A., Mebert, K., Koehler, G., Lotzkat, S., Ponce, M., & Vesely, M. (2014). Two new fringe-limbed frogs of the genus *Ecnomiohyla* (Anura: Hylidae) from Panama. *Zootaxa*, 3826(3), 449–474. <https://doi.org/10.11646/zootaxa.3826.3.2>

Bauer, A. M. (1989). Extracranial endolymphatic sacs in *Eurydactyloides* (Reptilia: Gekkonidae), with comments on endolymphatic function in lizards. *Journal of Herpetology*, 23(2), 172–175. <https://doi.org/10.2307/1564025>

Bauer, A. M. (2013). *Geckos: The animal answer guide*. Baltimore, MD: The Johns Hopkins University Press.

Bauer, A. M., & Russell, A. P. (1989). Supraorbital ossifications in geckos (Reptilia: Gekkonidae). *Canadian Journal of Zoology*, 67(3), 678–684. <https://doi.org/10.1139/z89-098>

Bellairs, d. A., & Kamal, A. M. (1981). The Chondrocranium and the development of the skull in recent reptiles. In C. Gans (Ed.), *Biology of the Reptilia* (Vol. 11, pp. 1–263). London, England: Academic Press.

Bever, G. S., Bell, C. J., & Maisano, J. A. (2005). The ossified braincase and cephalic osteoderms of *Shinisaurus crocodilurus* (Squamata, Shinisauridae). *Palaeontologia Electronica*, 8(1), 1–36.

Bhullar, B.-A. S., & Bell, C. J. (2008). Osteoderms of the California legless lizard *Anniella* (Squamata: Anguidae) and their relevance for considerations of miniaturization. *Copeia*, 2008(4), 785–793. <https://doi.org/10.1643/CG-07-189>

Broeckhoven, C., Diedericks, G., & Mouton, P. I. F. N. (2015). What doesn't kill you might make you stronger: Functional basis for variation in body armour. *Journal of Animal Ecology*, 84(5), 1213–1221. <https://doi.org/10.1111/1365-2656.12414>

Broeckhoven, C., du Plessis, A., & Hui, C. (2017). Functional trade-off between strength and thermal capacity of dermal armor: Insights from girdled lizards. *Journal of the Mechanical Behavior of Biomedical Materials*, 74, 189–194. <https://doi.org/10.1016/j.jmbbm.2017.06.007>

Broeckhoven, C., du Plessis, A., Minne, B., & Van Damme, R. (2019). Evolutionary morphology of osteoderms in squamates. *Journal of Morphology*, 280(S1), S90–S244. <https://doi.org/10.1002/jmor.21003>

Broeckhoven, C., El Adak, Y., Hui, C., Van Damme, R., & Stankowich, T. (2018). On dangerous ground: The evolution of body armour in cordyline lizards. *Proceedings of the Royal Society B: Biological Sciences*, 285(1880), 20180513. <https://doi.org/10.1098/rspb.2018.0513>

Broeckhoven, C., Mouton, P. I. F. N., & Hui, C. (2018). Proximate causes of variation in dermal armour: Insights from armadillo lizards. *Oikos*, 127 (10), 1449–1458. <https://doi.org/10.1111/oik.05401>

Buchwitz, M., & Voigt, S. (2010). Peculiar carapace structure of a Triassic chroniosuchian implies evolutionary shift in trunk flexibility. *Journal of Vertebrate Paleontology*, 30(6), 1697–1708. <https://doi.org/10.1080/02724634.2010.521685>

Buchwitz, M., Witzmann, F., Voigt, S., & Golubev, V. (2012). Osteoderm microstructure indicates the presence of a crocodylian-like trunk bracing system in a group of armoured basal tetrapods. *Acta Zoologica*, 93 (3), 260–280. <https://doi.org/10.1111/j.1463-6395.2011.00502.x>

Bucol, A., & Alcala, A. (2013). Tokay gecko, *Gekko gecko* (Sauria: Gekkonidae) predation on juvenile house rats. *Herpetology Notes*, 6, 307–308.

Burbrink, F. T., Graziotin, F. G., Pyron, R. A., Cundall, D., Donnellan, S., Irish, F., ... Zaher, H. (2019). Interrogating genomic-scale data for Squamata (lizards, snakes, and amphisbaenians) shows no support for key traditional morphological relationships. *Systematic Biology*, syz062. <https://doi.org/10.1093/sysbio/syz062>

Camp, C. L. (1923). Classification of the lizards. *Bulletin of the American Museum of Natural History*, 48, 289–482.

Campos, L. A., Da Silva, H. R., & Sebben, A. (2010). Morphology and development of additional bony elements in the genus *Brachycephalus*

(Anura: Brachycephalidae). *Biological Journal of the Linnean Society*, 99(4), 752–767. <https://doi.org/10.1111/j.1095-8312.2010.01375.x>

Carranza, S., Arnold, E. N., Mateo, J. A., & Geniez, P. (2002). Relationships and evolution of the north African geckos, *Geckonia* and *Tarentola* (Reptilia: Gekkonidae), based on mitochondrial and nuclear DNA sequences. *Molecular Phylogenetics and Evolution*, 23(2), 244–256. [https://doi.org/10.1016/S1055-7903\(02\)00024-6](https://doi.org/10.1016/S1055-7903(02)00024-6)

Carranza, S., Arnold, E. N., Mateo, J. A., & López-Jurado, L. F. (2000). Long-distance colonization and radiation in gekkonid lizards, *Tarentola* (Reptilia: Gekkonidae), revealed by mitochondrial DNA sequences. *Proceedings of the Royal Society of London B: Biological Sciences*, 267(1444), 637–649. <https://doi.org/10.1098/rspb.2000.1050>

Chen, I. H., Kiang, J. H., Correa, V., Lopez, M. I., Chen, P.-Y., McKittrick, J., & Meyers, M. A. (2011). Armadillo armor: Mechanical testing and micro-structural evaluation. *Journal of the Mechanical Behavior of Biomedical Materials*, 4(5), 713–722. <https://doi.org/10.1016/j.jmbbm.2010.12.013>

Chen, I. H., Yang, W., & Meyers, M. A. (2015). Leatherback Sea turtle shell: A tough and flexible biological design. *Acta Biomaterialia*, 28, 2–12. <https://doi.org/10.1016/j.actbio.2015.09.023>

Conrad, J. L. (2008). Phylogeny and systematics of Squamata (Reptilia) based on morphology. *Bulletin of the American Museum of Natural History*, 310, 1–182. <https://doi.org/10.1206/310.1>

Conrad, J. L., & Daza, J. D. (2015). Naming and rediagnosing the Cretaceous gekkonomorph (Reptilia, Squamata) from Öösh (Övörkhангай, Mongolia). *Journal of Vertebrate Paleontology*, 35(5), e980891. <https://doi.org/10.1080/02724634.2015.980891>

Conrad, J. L., Head, J. J., & Carrano, M. T. (2014). Unusual soft-tissue preservation of a crocodile lizard (Squamata, Shinisauria) from the Green River formation (Eocene) and shinisaur relationships. *The Anatomical Record*, 297(3), 545–559. <https://doi.org/10.1002/ar.22868>

Costantini, D., Alonso, M. L., Moazen, M., & Bruner, E. (2010). The relationship between cephalic scales and bones in lizards: A preliminary microtomographic survey on three lacertid species. *The Anatomical Record: Advances in Integrative Anatomy and Evolutionary Biology*, 293(2), 183–194. <https://doi.org/10.1002/ar.21048>

Curry Rogers, K., D'emic, M., Rogers, R., Vickaryous, M., & Cagan, A. (2011). Sauropod dinosaur osteoderms from the late cretaceous of Madagascar. *Nature Communications*, 2, 564. <https://doi.org/10.1038/ncomms1578>

Dacke, C. G., Elsey, R. M., Trosclair, P. L., III, Sugiyama, T., Nevarez, J. G., & Schweitzer, M. H. (2015). Alligator osteoderms as a source of labile calcium for eggshell formation. *Journal of Zoology*, 297(4), 255–264. <https://doi.org/10.1111/jzo.12272>

Daza, J. D., Herrera, A., Thomas, R., & Claudio, H. J. (2009). Are you what you eat? A geometric morphometric analysis of gekkotan skull shape. *Biological Journal of the Linnean Society*, 97(3), 677–707. <https://doi.org/10.1111/j.1095-8312.2009.01242.x>

Daza, J. D., Mapps, A. A., Lewis, P. J., Thies, M. L., & Bauer, A. M. (2015). Peramorphic traits in the Tokay gecko skull. *Journal of Morphology*, 276(8), 915–928. <https://doi.org/10.1002/jmor.20389>

de Queiroz, K. (1987). *Phylogenetic systematics of iguanine lizards: A comparative osteological study* (p. 118). Berkeley, CA: University of California Press.

Dilkes, D., & Brown, L. E. (2007). Biomechanics of the vertebrae and associated osteoderms of the early Permian amphibian *Cacops aspidophorus*. *Journal of Zoology*, 271(4), 396–407. <https://doi.org/10.1111/j.1469-7998.2006.00221.x>

Erickson, G. M., De Ricqlès, A., De Buffrénil, V., Molnar, R. E., & Bayless, M. K. (2003). Vermiform bones and the evolution of gigantism in *Megalania*—How a reptilian fox became a lion. *Journal of Vertebrate Paleontology*, 23(4), 966–970. <https://doi.org/10.1671/23>

Estes, R., de Queiroz, K., & Gauthier, J. A. (1988). Phylogenetic relationships within Squamata. In *Phylogenetic relationships of the lizard families* (pp. 119–281). Standford, CA: Standford University Press.

Evans, S. E. (2008). The skull of lizards and tuatara. In C. Gans, A. S. Gaunt, & K. Adler (Eds.), *Biology of the Reptilia, the skull of Lepidosauria* (Vol. 20, pp. 1–347). Ithaca, NY: The Society for the Study of Amphibians and Reptiles (SSAR).

Farlow, J. O., Hayashi, S., & Tattersall, G. J. (2010). Internal vascularity of the dermal plates of *Stegosaurus* (Ornithischia, Thyreophora). *Swiss Journal of Geosciences*, 103(2), 173–185. <https://doi.org/10.1007/s00015-010-0021-5>

Farlow, J. O., Thompson, C. V., & Rosner, D. E. (1976). Plates of the dinosaur *Stegosaurus*: Forced convection heat loss fins? *Science*, 192(4244), 1123–1125. <https://doi.org/10.1126/science.192.4244.1123>

Fitch, H. S. (1981). *Sexual size differences in reptiles*. Miscellaneous publication - University of Kansas, Museum of Natural History, 70, 1–72.

Frey, E. (1988). The carrying system of crocodilians—A biomechanical and phylogenetical analysis. *Stuttgarter Beiträge zur Naturkunde Serie A (Biologie)*, 426, 1–60.

Gadow, H. (1901). *Cambridge natural history: Amphibia and Reptiles* (Vol. VIII). New York, NY: Hafner Publishing Company.

Gao, K., & Norell, M. A. (2000). Taxonomic composition and systematics of Late Cretaceous lizard assemblages from Ukhaa Tolgod and adjacent localities, Mongolian Gobi Desert. *Bulletin of the American Museum of Natural History*, 2000(249), 1–118. [https://doi.org/10.1206/0003-0090\(2000\)249<0001:TCASOL>2.0.CO;2](https://doi.org/10.1206/0003-0090(2000)249<0001:TCASOL>2.0.CO;2)

Good, D. A., & Schwenk, K. (1985). A new species of *Abrovia* (Lacertilia: Anguidae) from Oaxaca, Mexico. *Copeia*, 1985(1), 135–141. <https://doi.org/10.2307/1444801>

Grafen, A. (1989). The phylogenetic regression. *Philosophical Transactions of the Royal Society of London. B: Biological Sciences*, 326(1233), 119–157. <https://doi.org/10.1098/rstb.1989.0106>

Griffing, A. H., Daza, J. D., DeBoer, J. C., & Bauer, A. M. (2018). Developmental osteology of the parafrontal bones of the sphaerodactylidae. *The Anatomical Record*, 301(4), 581–606. <https://doi.org/10.1002/ar.23749>

Harmon, L. J., Weir, J. T., Brock, C. D., Glor, R. E., & Challenger, W. (2008). GEIGER: Investigating evolutionary radiations. *Bioinformatics*, 24(1), 129–131. <https://doi.org/10.1093/bioinformatics/btm538>

Henkel, F.-W., & Schmidt, J. (1995). *Geckoes: Biology, husbandry and reproduction*. Malabar, FL: Krieger Publishing Company.

Hill, R. V. (2005). Integration of morphological data sets for phylogenetic analysis of Amniota: The importance of integumentary characters and increased taxonomic sampling. *Systematic Biology*, 54(4), 530–547. <https://doi.org/10.1080/10635150590950326>

Hofstetter, R., & Gasc, J. P. (1969). Vertebrae and ribs of modern reptiles. In C. Gans, D. A. Bellairs, & T. S. Parsons (Eds.), *Biology of the Reptilia* (Vol. 1, pp. 201–301). London, England: Academic Press.

Katoh, K., & Standley, D. M. (2013). MAFFT multiple sequence alignment software version 7: Improvements in performance and usability. *Molecular Biology and Evolution*, 30(4), 772–780. <https://doi.org/10.1093/molbev/mst010>

King, D. (1964). The osteology of the water skink, *Lygosoma (Sphenomorphus) quoyii*. *Australian Journal of Zoology*, 12(2), 201–216. <https://doi.org/10.1071/ZO9640201>

Klein, N., Scheyer, T., & Tütken, T. (2009). Skeletochronology and isotopic analysis of a captive individual of *Alligator mississippiensis* Daudin, 1802. *Fossil Record*, 12(2), 121–131. <https://doi.org/10.1002/mmng.200900002>

Kluge, A. G. (1967). Higher taxonomic categories of Gekkonid lizards and their evolution. *Bulletin of the American Museum of Natural History*, 135(1), 1–60.

Kraft, R. (1995). Xenarthra. In J. Niethammer, H. Schliemann, & D. Starck (Eds.), *Handbuch der Zoologie* (Vol. 8). Berlin, Germany: Walter de Gruyter.

Krause, D. W., Evans, S. E., & Gao, K.-Q. (2003). First definitive record of Mesozoic lizards from Madagascar. *Journal of Vertebrate Paleontology*, 23(4), 842–856. <https://doi.org/10.1671/23>

Krmpotic, C. M., Ciancio, M. R., Carlini, A. A., Castro, M. C., Scarano, A. C., & Barbeito, C. G. (2015). Comparative histology and ontogenetic change in the carapace of armadillos (Mammalia: Dasypodidae). *Zoomorphology*, 134(4), 601–616. <https://doi.org/10.1007/s00435-015-0281-8>

Lamb, A. D., Watkins-Colwell, G. J., Moore, J. A., Warren, D. L., Iglesias, T. L., Brandley, M. C., & Dornburg, A. (2017). Endolymphatic sac use and reproductive activity in the Lesser Antilles endemic gecko *Gonatodes antillensis* (Gekkota: Sphaerodactylidae). *Bulletin of the Peabody Museum of Natural History*, 58(1), 17–30. <https://doi.org/10.3374/014.058.0103>

Lanfear, R., Frandsen, P. B., Wright, A. M., Senfeld, T., & Calcott, B. (2016). PartitionFinder 2: New methods for selecting partitioned models of evolution for molecular and morphological phylogenetic datasets. *Molecular Biology and Evolution*, 34(3), 772–773. <https://doi.org/10.1093/molbev/msw260>

Levrat-Calviac, V. (1986). Étude comparée des ostéoderms de *Tarentola mauritanica* et de *T. neglecta* (Gekkonidae, Squamata). *Archives d'Anatomie Microscopique et de Morphologie Expérimentale*, 75(1), 29–43.

Levrat-Calviac, V., & Zylberberg, L. (1986). The structure of the osteoderms in the gekko: *Tarentola mauritanica*. *American Journal of Anatomy*, 176(4), 437–446. <https://doi.org/10.1002/aja.1001760406>

Loveridge, A. (1947). Revision of the African lizards of the family Gekkonidae. *Bulletin of the Museum of Comparative Zoology*, 98, 1–469.

Maisano, J. A. (2002). Terminal fusions of skeletal elements as indicators of maturity in squamates. *Journal of Vertebrate Paleontology*, 22(2), 268–275. [https://doi.org/10.1671/0272-4634\(2002\)022\[0268:TFOSEA\]2.0.CO;2](https://doi.org/10.1671/0272-4634(2002)022[0268:TFOSEA]2.0.CO;2)

Maisano, J. A., Bell, C. J., Gauthier, J. A., & Rowe, T. (2002). The osteoderms and palpebral in *Lanthanotus borneensis* (Squamata: Anguimorpha). *Journal of Herpetology*, 36(4), 678–683. [https://doi.org/10.1670/0022-1511\(2002\)036\[0678:TOAPIL\]2.0.CO;2](https://doi.org/10.1670/0022-1511(2002)036[0678:TOAPIL]2.0.CO;2)

Maisano, J. A., Leduc, T. J., Bell, C. J., & Barber, D. (2019). The cephalic osteoderms of *Varanus komodoensis* as revealed by high-resolution X-ray computed tomography. *The Anatomical Record*, 302, 1675–1680. <https://doi.org/10.1002/ar.24197>

Mangione, S., & Montero, R. (2001). The endolymphatic sacs in embryos of *Amphisbaena Darwini*. *Journal of Herpetology*, 35(3), 524–529. <https://doi.org/10.2307/1565977>

Marcellini, D. (1977). Acoustic and visual display behavior of gekkonid lizards. *American Zoologist*, 17(1), 251–260. <https://doi.org/10.1093/icb/17.1.251>

Martins, E. P., & Hansen, T. F. (1997). Phylogenies and the comparative method: A general approach to incorporating phylogenetic information into the analysis of interspecific data. *The American Naturalist*, 149(4), 646–667. <https://doi.org/10.1086/286013>

McConnachie, S., & Whiting, M. J. (2003). Costs associated with tail autotomy in an ambush foraging lizard, *Cordylus melanotus melanotus*. *African Zoology*, 38(1), 57–65. <https://doi.org/10.1080/15627020.2003.11657194>

McDowell, S. B., & Bogert, C. M. (1954). The systematic position of *Lanthanotus* and the affinities of the anguinomorphan lizards. *Bulletin of the American Museum of Natural History*, 105, 1–142.

Moss, M. L. (1969). Comparative histology of dermal sclerifications in reptiles. *Acta Anatomica*, 73(4), 510–533. <https://doi.org/10.1159/000143315>

Nguyen, L.-T., Schmidt, H. A., von Haeseler, A., & Minh, B. Q. (2015). IQ-TREE: A fast and effective stochastic algorithm for estimating maximum-likelihood phylogenies. *Molecular Biology and Evolution*, 32(1), 268–274. <https://doi.org/10.1093/molbev/msu300>

Niethammer, J. (1975). Hautverknöcherungen im schwanz von stachelmäusen (*Acromys dimidiatus*). *Bonner Zoologische Beiträge*, 26(1–3), 100–106.

Oliver, J. A. (1951). Ontogenetic changes in osteodermal ornamentation in skinks. *Copeia*, 1951(2), 127–130. <https://doi.org/10.2307/1437541>

Otto, H., & Coburg, S. (1909). Die Beschuppung der Brevilinguier und Ascalaboten. *Jenaische Zeitschrift für Naturwissenschaft*, 37, 193–252.

Paluh, D. J., & Bauer, A. M. (2017). Comparative skull anatomy of terrestrial and crevice-dwelling *Trachylepis* skinks (Squamata: Scincidae) with a survey of resources in scincid cranial osteology. *PLoS One*, 12(9), e0184414. <https://doi.org/10.1371/journal.pone.0184414>

Paluh, D. J., Griffing, A. H., & Bauer, A. M. (2017). Sheddable armour: Identification of osteoderms in the integument of *Geckolepis maculata* (Gekkota). *African Journal of Herpetology*, 66(1), 12–24. <https://doi.org/10.1080/21564574.2017.1281172>

Paradis, E., & Schliep, K. (2018). Ape 5.0: An environment for modern phylogenetics and evolutionary analyses in R. *Bioinformatics*, 35, 526–528. <https://doi.org/10.1093/bioinformatics/bty633>

Parker, H. W., & Taylor, R. H. R. (1942). The lizards of British Somaliland. *Bulletin of the Museum of Comparative Zoology*, 91, 1–101.

Petzold, H.-G. (2007). Lives of captive reptiles—Translation of “Aufgaben und Probleme bei der Erforschung der Lebensäußerungen der Niederen Amnioten (Reptilien)” [Tasks and Problems Encountered by Zoo Keepers in Research Concerning the Vital Manifestations of the Lower Amniotic Animals (Reptiles)] (Translated by L. Heichler and J.B. Murphy) (Vol. 22). Ithaca, NY: Society for the Study of Amphibians and Reptiles (SSAR).

R Core Team. (2012). *R: A language and environment for statistical computing*. Vienna: R Foundation for Statistical Computing Retrieved from <http://www.R-project.org>

Rasband, W. S. (2018). *US Image J*. Bethesda, MD: National Institutes of Health Retrieved from <https://imagej.nih.gov/ij/>

Read, R. (1986). *Osteoderms in the Lacertilia: An investigation into the structure and phylogenetic implications of dermal bone found under the skin of lizards* (PhD thesis), California State University, Fullerton, CA.

Romer, A. S. (1956). *Osteology of the reptiles*. Chicago, IL: University of Chicago Press.

Rösler, H., Bauer, A. M., Heinicke, M. P., Greenbaum, E., Jackman, T., Nguyen, T. Q., & Ziegler, T. (2011). Phylogeny, taxonomy, and zoogeography of the genus *Gekko* Laurenti, 1768 with the revalidation of *G. reevesii* Gray, 1831 (Sauria: Gekkonidae). *Zootaxa*, 2989(1), 1–50. <https://doi.org/10.11646/zootaxa.2989.1.1>

Ruibal, R., & Shoemaker, V. (1984). Osteoderms in anurans. *Journal of Herpetology*, 18, 313–328. <https://doi.org/10.2307/1564085>

Russell, A. P., & Bauer, A. M. (1987). Le gecko géant *Hoplodactylus delcourti* et ses relations avec le gigantisme et l'endémisme insulaire chez les Gekkonidae. *Mésogée*, 46, 25–28.

Russell, A. P., Vickaryous, M. K., & Bauer, A. M. (2016). The phylogenetic distribution, anatomy and histology of the post-cloacal bones and adnexa of geckos. *Journal of Morphology*, 277(2), 264–277. <https://doi.org/10.1002/jmor.20494>

Scherz, M. D., Daza, J. D., Köhler, J., Vences, M., & Glaw, F. (2017). Off the scale: A new species of fish-scale gecko (Squamata: Gekkonidae: *Geckolepis*) with exceptionally large scales. *PeerJ*, 5, e2955. <https://doi.org/10.7717/peerj.2955>

Schmidt, W. J. (1911). Beobachtungen an der Haut von *Geckolepis* und einigen anderen Geckoniden. In A. Voeltzkow (Ed.), *Reise in Ostafrika in den Jahren 1903–1905 mit Mitteln der Hermann und Elise geb. Hickman Wentzel-Stiftung ausgeführt Wissenschaftliche Ergebniss von Alfred Voeltzkow* (Vol. 4, pp. 331–352). Stuttgart, BW: Schweizerbart'sche Verlagsbuchhandlung.

Schmidt, W. J. (1912). Studien am Integument der Reptilien. I. Die Haut der Geckoniden. *Zeitschrift für Wissenschaftliche Zoologie*, 51, 139–258.

Schucht, P. J., Rühr, P. T., Geier, B., Glaw, F., & Lambertz, M. (2019). Armored with skin and bone: The integumentary morphology of the Antsingy leaf chameleon *Brookesia perarmata* (Iguania: Chamaeleonidae). *Journal of Morphology*, 280(S1), S214–S244. <https://doi.org/10.1002/jmor.21003>

Seidel, M. R. (1979). The osteoderms of the American alligator and their functional significance. *Herpetologica*, 35(4), 375–380.

Seufer, H. (1991). *Keeping and breeding geckos*. Neptune, NJ: TFH Publications.

Siebenrock, F. (1893). Das Skelet von *Brookesia superciliaris* Kuhl. *Sitzungsberichte der Mathematisch-Naturwissenschaftlichen Classe der Kaiserlichen Akademie der Wissenschaften*, 102, 71–118.

Siebenrock, F. (1894). Das Skelet der *Lacerta simonyi* Steind. und der Lacertiden familie überhaupt. *Sitzungsberichte der Kaiserlichen Akademie der Wissenschaften Math.-naturw.*, Klasse Abt. 1, 103, 205–292.

Simoes, T. R., Caldwell, M. W., Tałanda, M., Bernardi, M., Palci, A., Vernygora, O., ... Nydam, R. L. (2018). The origin of squamates revealed by a middle Triassic lizard from the Italian Alps. *Nature*, 557 (7707), 706–709. <https://doi.org/10.1038/s41586-018-0093-3>

Stanley, E. L. (2013). *Systematics and morphological diversification of the Cordylidae (Squamata)* (PhD Doctoral dissertation), American Museum of Natural History, New York, NY. Retrieved from <http://digitallibrary.amnh.org/handle/2246/6713>

Stanley, E. L., Paluh, D. J., & Blackburn, D. C. (2019). Diversification of dermal armor in squamates. *Journal of Morphology*, 280(S1), S224–S244. <https://doi.org/10.1002/jmor.21003>

Suchard, M. A., Lemey, P., Baele, G., Ayres, D. L., Drummond, A. J., & Rambaut, A. (2018). Bayesian phylogenetic and phylodynamic data integration using BEAST 1.10. *Virus Evolution*, 4(1), vey016. <https://doi.org/10.1093/ve/vey016>

Sun, C.-Y., & Chen, P.-Y. (2013). Structural design and mechanical behavior of alligator (*Alligator mississippiensis*) osteoderms. *Acta Biomaterialia*, 9 (11), 9049–9064. <https://doi.org/10.1016/j.actbio.2013.07.016>

Symonds, M. R. E., & Blomberg, S. P. (2014). A primer on phylogenetic generalised least squares. In L. Z. Garamszegi (Ed.), *Modern phylogenetic comparative methods and their application in evolutionary biology* (pp. 105–130). Berlin, Heidelberg: Springer-Verlag.

Uetz, P., Freed, P., & Hošek, J. (2019). The Reptile Database. Retrieved from <http://www.reptile-database.org>

Vickaryous, M. K., & Hall, B. K. (2006). Osteoderm morphology and development in the nine-banded armadillo, *Dasypus novemcinctus* (Mammalia, Xenarthra, Cingulata). *Journal of Morphology*, 267(11), 1273–1283. <https://doi.org/10.1002/jmor.10475>

Vickaryous, M. K., Meldrum, G., & Russell, A. P. (2015). Armored geckos: A histological investigation of osteoderm development in *Tarentola* (Phyllodactylidae) and *Gekko* (Gekkonidae) with comments on their regeneration and inferred function. *Journal of Morphology*, 276(11), 1345–1357. <https://doi.org/10.1002/jmor.20422>

Vickaryous, M. K., & Sire, J. Y. (2009). The integumentary skeleton of tetrapods: Origin, evolution, and development. *Journal of Anatomy*, 214(4), 441–464. <https://doi.org/10.1111/j.1469-7580.2008.01043.x>

Villa, A., Daza, J. D., Bauer, A. M., & Delfino, M. (2018). Comparative cranial osteology of European gekkotans (Reptilia, Squamata). *Zoological Journal of the Linnean Society*, 184(3), 857–895. <https://doi.org/10.1093/zoolinnean/zlx104>

von Koenigswald, W., & Storch, G. (1983). *Pholidocercus hassiacus*, ein Amphilemuride aus dem Eözan der "Grube Messel" bei Darmstadt (Mammalia, Lipotyphla). *Senckenbergiana Lethaea*, 64, 447–495.

Whiteside, B. (1922). The development of the *saccus endolymphaticus* in *Rana temporaria* Linné. *The American Journal of Anatomy*, 30(2), 231–266. <https://doi.org/10.1002/aja.1000300204>

Wood, P. L. J., Guo, X., Travers, S. L., Su, Y.-C., Olson, K. V., Bauer, A. M., ... Brown, R. M. (2019). Parachute geckos free fall into synonymy: *Gekko* phylogeny, and a new subgeneric classification, inferred from thousands of ultraconserved elements. *bioRxiv*, 717520. <https://doi.org/10.1101/717520>

Zylberberg, L., & Castanet, J. (1985). New data on the structure and the growth of the osteoderms in the reptile *Anguis fragilis* L. (Anguidae, Squamata). *Journal of Morphology*, 186(3), 327–342. <https://doi.org/10.1002/jmor.1051860309>

SUPPORTING INFORMATION

Additional supporting information may be found online in the Supporting Information section at the end of this article.

How to cite this article: Laver RJ, Morales CH, Heinicke MP, et al. The development of cephalic armor in the tokay gecko (Squamata: Gekkonidae: *Gekko gecko*). *Journal of Morphology*. 2020;281:213–228. <https://doi.org/10.1002/jmor.21092>